A counterpoise design for RF-induced heating reduction

Yu Wang, Jianfeng Zheng, Member, IEEE, Qingyan Wang, and Ji Chen, Senior Member, IEEE

Abstract—This paper presents a novel lead body design for active implantable medical devices (AIMD) to reduce Radio-frequency (RF) induced heating during magnetic resonance imaging (MRI) scanning. By introducing a counterpoise electrode to the original lead construct, part of the RF-induced energy can be decoyed into the surrounding tissues while the therapy signal is intact. The numerical simulation studies of three leads with different configurations are presented to demonstrate the effectiveness of this technique. From simulation results at 1.5 T, the peak 1g average SAR value can be reduced by a factor of 3 when the length of the counterpoise electrode is properly designed.

Clinical Relevance—With this novel AIMD design technique, the AIMDs can be designed safer under the MRI environment.

I. Introduction

Magnetic resonance imaging (MRI) compatibility assessment for active implantable medical devices (AIMD) is an essential stage before AIMDs can be approved for clinical usage. The radiofrequency (RF)-induced heating, caused by the interactions between the MRI RF coil and the AIMDs containing the metallic components, is one of the major concerns. Due to the high risk of RF-induced heating which can damage the human tissue, there is an increasing number of investigations aiming at the heating reduction for AIMD using diverse methods.

The efforts on the heating reduction for implantable devices under RF field mainly can be classified into two categories: one is to change the device exposure environment, such as incident field reduction, to reduce the device heating[1]-[10]; the other approach is to modify the designs of AIMD to effectively suppress the RF-induced heating[11]-[24].

Two typical approaches were used in the design modification for device heating reduction. The first one is to modify the stimulation electrodes geometry, such as increasing the resistance of the electrode at radio-frequency by an appropriate winding method[22], changing the insulation layer materials[20], introducing filters[14]-Error! Reference source not found, and adding high-dielectric materials[19].

^Ji Chen is with the Department of Electrical and Computer Engineering, University of Houston, TX 77204-4005 USA (corresponding author e-mail: jchen23@central.uh.edu)

Yu Wang is with the Department of Electrical and Computer Engineering, University of Houston, TX 77204-4005 USA (ywang129@uh.edu)

Jianfeng Zheng is with the Department of Electrical and Computer Engineering, University of Houston, TX 77204-4005 USA (jzheng4@central.uh.edu)

Qingyan Wang is with the Department of Electrical and Computer Engineering, University of Houston, TX 77204-4005 USA (qwang25@uh.edu)

The other approach is to modify the tip electrode structure, such as enlarging the pin area[17][21][25], or adding lumped elements to changing the termination impedance[12].

In this paper, we propose a novel lead body design technique by introducing a counterpoise electrode to decoy a portion of the induced energy into the surrounding tissues. This electrode, which is referred to as the counterpoise electrode will not impair the therapy signal. It is demonstrated that when the length of the counterpoise electrode is properly designed, it can reduce the RF-induced heating by a factor over 3.

II. METHODOLOGY

A. AIMD structure with counterpoise electrode

The AIMDs comprised of an implantable pulse generator (IPG), elongated leads body with one or more metallic electrodes to deliver therapy signals, and leads tip electrodes contacting with human tissue to be stimulated. In Fig. 1(a), a generic structure of AIMD with a single stimulation electrode connecting to the leads tip electrode is presented. A feedthrough capacitor is added between the stimulation electrode and the IPG metal shell to filter out undesired electrical interference. The stimulation electrode construct has a helix structure encapsulated by an insulation layer. In Fig. 1(b), the generic structure of AIMD with an extra counterpoise electrode is presented. The red stimulation electrode is used to deliver the therapy signal to human tissue while the blue counterpoise electrode is introduced to the original construct and is connected with five counterpoise pins at both ends. Since there is no direct electrode contact, the therapy signal will not be altered (a feedthrough capacitor, stimulation electrode, and tip electrode); however, this construct can couple some of the RF-induced energy from the stimulation electrode and dissipate the energy into the human tissue through counterpoise pins. Consequently, the overall energy induced at the stimulus tip electrode can be reduced.

The AIMD implanted in human tissue could be represented as a transmission line system with terminations modeled as lumped elements, as Fig. 2 (a) shows. In Fig. 2 (b), with the addition of the counterpoise electrode, the system can be represented by a multi-transmission line model. When the AIMD is under the RF incident field, induced energy on the original electrode can be coupled onto the counterpoise electrode and dissipated into the surrounding tissue through the counterpoise pins with larger surface area. Therefore, the energy deposition at the tip electrode of the original lead could be significantly mitigated.

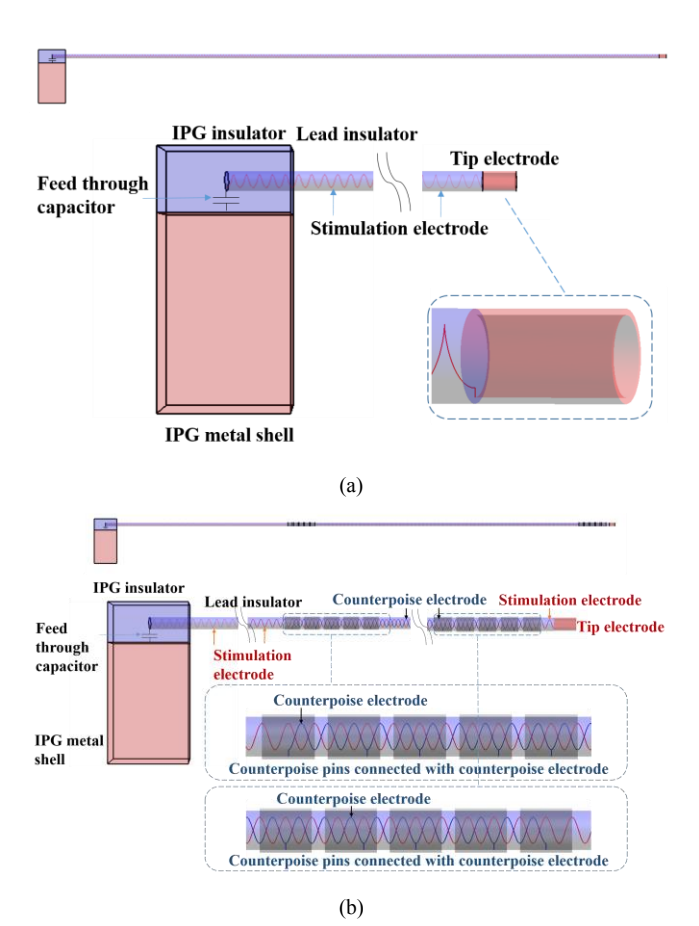


Fig. 1 (a) The generic structure of AIMD with one electrode for stimulation, connecting with a tip electrode. (b) The generic structure of AIMD with an extra counterpoise electrode to depress the RF-induced heating, connecting with counterpoise pins.

B. The circuit model of the AIMD with counterpoise electrode

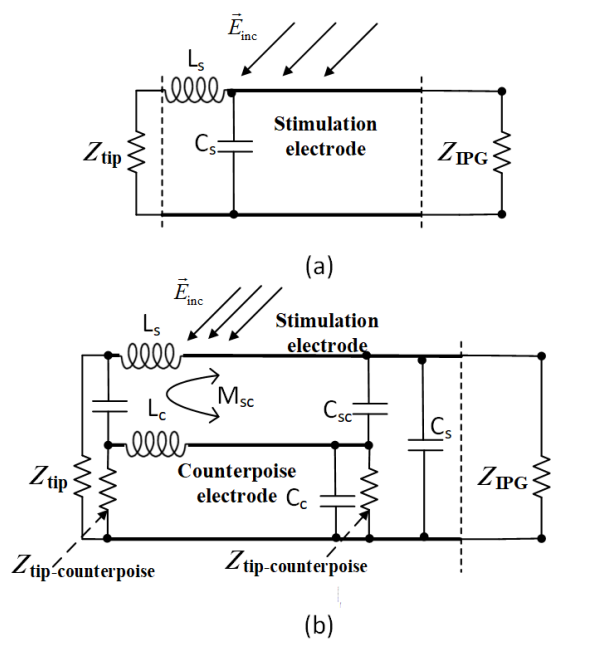


Fig. 2 (a) The circuit model of AIMD with only stimulation system to deliver therapy signal; (b) the circuit model of AIMD with stimulation system and counterpoise electrode to reduce the RF-induced heating.

III. NUMERICAL SIMULATION RESULT

Numerical simulations were conducted to demonstrate this design. The simulations were performed using the SEMCAD X software package, which applies the finite-difference time-domain (FDTD) method to solve complex problems. For the 1.5 T MRI system, the operating frequency is 64 MHz. A generic tuned birdcage coil was used to generate the incident electromagnetic field, as shown in Fig. 3. The diameter of the RF birdcage coil was 630 mm and the height was 650 mm. A linear polarized electromagnetic field distribution inside the birdcage coil was achieved, excited by eight current sources on each rung. The ASTM phantom filled with saline conductivity of 0.47 S/m and relative permittivity at 78 was used to mimic the implantation environment of AIMD.

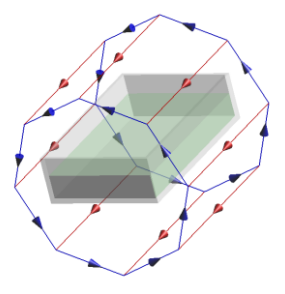


Fig. 3. Illustration of the 1.5 T generic birdcage coil used in the study.

Three case studies have been performed to demonstrate the effectiveness of the counterpoise electrode on suppressing the RF-induced heating. Three controlled leads with a single conductor and the same leads tip electrode and the IPG but different leads structures were used. The radius of the insulator was 1.5 mm. The detailed parameters of the three controlled leads are shown in Table I.

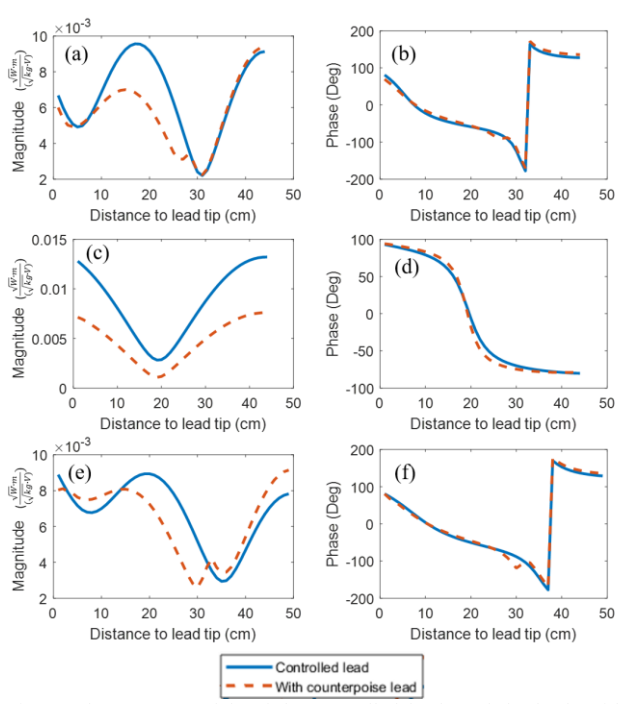


Fig. 4. The AIMD models of the controlled leads and the leads with the introducing of counterpoise leads, (a) Magnitude and (b) phase for leads 1; (c)(d) are for the leads 2 and its modified leads; (e)(f) are for the leads 3 and its modified leads.

TABLE I. THE PARAMETERS OF THE CONTROLLED LEADS WITH SINGLE HELIX CONDUCTOR

	Helix leads radius (mm)	Helix leads turn distance (mm)	ϵ_r of leads insulator	Total leads length (cm)
Leads 1	1	2	3.7	45
Leads 2	0.5	2	3.7	45
Leads 3	1	5	10	50

For each of the three leads, the counterpoise electrode has the same helix leads radius, turn distance, and leads insulator as the original leads. It was observed the length of the counterpoise leads can have a significant effect on the induced heating. In the following part, the lengths of the counterpoise electrode for three leads are chosen to be 28 cm, 44 cm, and 33 cm, respectively.

The original AIMD models (i.e., the transfer functions) for three pairs of leads are determined using the method described in [26]. The results are presented in Fig. 4. It can be seen that the magnitudes of the AIMDs model have been reduced. This indicates the new designs would lead to lower RF-induced heating during MRI procedures.

The RF-induced heating is evaluated when the original leads were placed at the 2 cm to the wall of the phantom, 4.5 cm under the surface of the gel. For the comparison, the leads with the counterpoise constructs placed at the same location were also studied. The comparison of the SAR distribution for the pair of leads 1 was presented in Fig. 5. It can be seen that the deposited power would be accumulated at the region of the tip electrode for the controlled leads. By introducing the counterpoise electrode, some of the RF-induced energy was coupled into the gel through counterpoise pins connected to the counterpoise electrode. Therefore, the induced energy at the leads tip electrode will be decreased significantly. The results for the other two leads are given in Fig. 6. The ratios of heating reduction were 74 %, 73 %, and 68 %, for the three cases, respectively. All results were normalized to 2 W/kg whole-body SAR value.

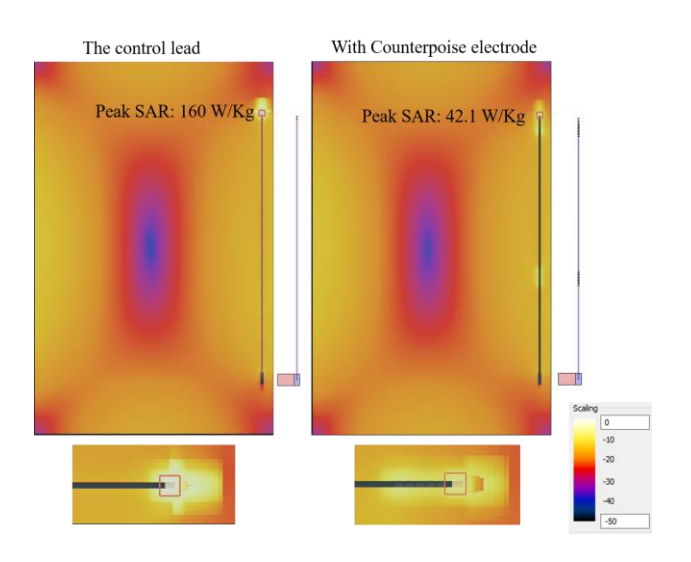


Fig. 5. The comparison of the SAR distribution for the controlled leads 1(left), and the leads 1 with counterpoise electrode (right). The zoom-in viewing of the SAR distribution at the lead tip electrode is presented at the bottom of the figure. All figures are normalized to the same dB scale.

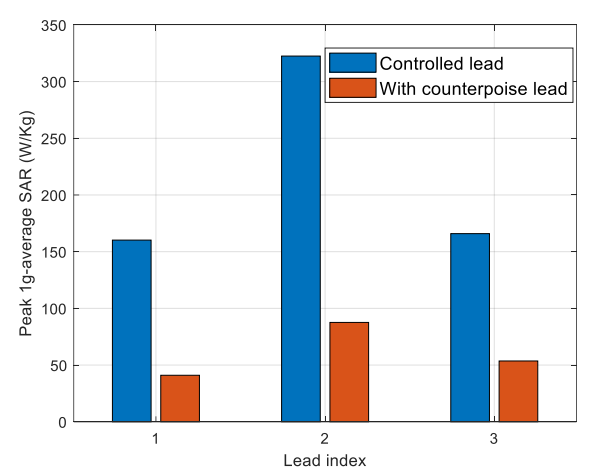


Fig. 6 The comparison of the peak 1g average SAR for the three pairs of the leads (controlled leads and the modified leads with the counterpoise electrode)

To demonstrate the relationship between the length of the counterpoise electrode and the heating suppression performance, three groups of the parameter sweeping studies were performed. The different lengths of the counterpoise electrode were studied. The simulation results are given in Fig. 7.

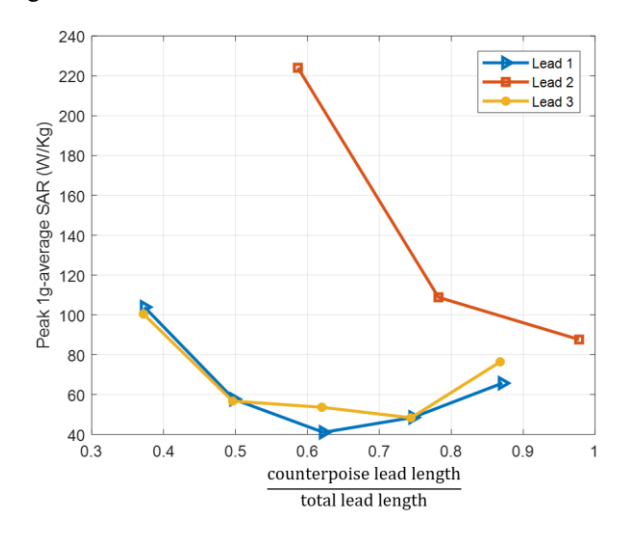


Fig. 7 The peak 1g average SAR for different lengths of the counterpoise electrodes

From Fig. 7, it is noticed that the lengths of the counterpoise electrode would significantly influence the performance of heating reduction. Therefore, the length of the counterpoise electrode needs to be designed carefully to achieve the optimal performance for RF-induced heating reduction.

IV. CONCLUSION

This paper presents a novel leads design for active implantable medical devices (AIMD) to reduce Radio-frequency (RF) induced heating when exposed to magnetic resonance imaging (MRI) scanning. By introducing a counterpoise electrode to the original leads structure, the RF-induced energy can be coupled out into the gel or human

tissue through pins connected to the counterpoise electrode, while the electrode designed to deliver the therapy signal (usually at low frequency compared to the RF pulses) will not be impacted. The numerical simulation studies of three leads with different configurations are presented to validate this design. From the simulation results at 1.5 T, the peak 1g average SAR decreased by a factor over 3 with 2 W/Kg whole body SAR in phantom.

REFERENCES

- [1] Y. Eryaman, B. Akin, and E. Atalar, "Reduction of implant RF heating through modification of transmit coil electric field," *Magn. Reson. Med.*, vol. 65, no. 5, pp. 1305–1313, 2011.
- [2] Y. Eryaman, E. A. Turk, C. Oto, O. Algin, and E. Atalar, "Reduction of the radiofrequency heating of metallic devices using a dual-drive birdcage coil," *Magn. Reson. Med.*, vol. 69, no. 3, pp. 845–852, 2013.
- [3] S. B. de Cardiologia et al., "Reconfigurable MRI coil technology can substantially reduce RF heating at the tips of bilateral deep brain stimulation impalnts, 2018.
- [4] T. Herrington et al., "Construction and modeling of a reconfigurable MRI coil for lowering SAR in patients with deep brain stimulation implants," *Neuroimage*, vol. 147, no. December 2016, pp. 577–588, 2017.
- [5] R. Yang, J. Zheng, Y. Wang, R. Guo, W. Kainz, and J. Chen, "An Absorbing Radio Frequency Shield to Reduce RF Heating Induced by Deep Brain Stimulator During 1.5-T MRI," *IEEE Trans. Electromagn. Compat.*, vol. PP, pp. 1–7, 2019.
- [6] E. Mattei, E. Lucano, F. Censi, L. M. Angelone, and G. Calcagnini, "High dielectric material in MRI: Numerical assessment of the reduction of the induced local power on implanted cardiac leads," *Proc. Annu. Int. Conf. IEEE Eng. Med. Biol. Soc. EMBS*, vol. 2016-Octob, pp. 2361–2364, 2016.
- [7] X. Huang et al., "MRI Heating Reduction for External Fixation Devices Using Absorption Material," *IEEE Trans. Electromagn. Compat.*, vol. 57, no. 4, pp. 635–642, 2015.
- [8] M. E. Ladd and H. H. Quick, "Reduction of resonant RF heating in intravascular catheters using coaxial chokes," *Magn. Reson. Med.*, vol. 43, no. 4, pp. 615–619, 2000.
- [9] L. Golestanirad, B. Keil, L. M. Angelone, G. Bonmassar, A. Mareyam, and L. L. Wald, "Feasibility of using linearly polarized rotating birdcage transmitters and close-fitting receive arrays in MRI to reduce SAR in the vicinity of deep brain simulation implants," *Magn. Reson. Med.*, vol. 77, no. 4, pp. 1701–1712, 2017.
- [10] C. E. McElcheran, B. Yang, K. J. T. Anderson, L. Golenstani-Rad, and S. J. Graham, "Investigation of parallel radiofrequency transmission for the reduction of heating in long conductive leads in 3 Tesla magnetic resonance imaging," *PLoS One*, vol. 10, no. 8, pp. 1–21, 2015.
- [11] A. C. Özen, T. Lottner, and M. Bock, "Safety of active catheters in MRI: Termination impedance versus RF-induced heating," *Magn. Reson. Med.*, vol. 81, no. 2, pp. 1412–1423, 2019.
- [12] J. Liu, D. R. Jackson, Q. Wang, W. Kainz, and J. Chen, "On the Relationship Between Impedances of Active Implantable Medical Devices and Device Safety Under MRI RF Emission," *IEEE Trans. Electromagn. Compat.*, vol. PP, pp. 1–9, 2019.
- [13] S. McCabe, J. Scott, and S. Butler, "Electromagnetic techniques to minimize the risk of hazardous local heating around medical implant electrodes during MRI scanning," Eur. Microw. Week 2015 "Freedom Through Microwaves", EuMW 2015 - Conf. Proceedings; 2015 45th Eur. Microw. Conf. Proceedings, EuMC, pp. 702–705, 2015.
- [14] Wahlstrand et al, "Lead Electrode for use in an MRI-safe implantable medical device", U.S. Patent 7174219, Feb. 6, 2007.
- [15] I. H. R. Halperin, R. A. Stevenson, A. Examiner, and M. D. Abreu, "Band stop filter comprising and inductive component disposed in a lead wire in series with an electrode", U.S. Patent 9248283, Feb. 2, 2016.
- [16] X. Min, "Systems and methods for determining inductance and capacitance values for use with LC filters within implantable medical device leads to reduce lead heating during MRI", U.S. Patent 9233240, Jan. 12, 2016.
- [17] R. Yang, J. Zheng, and J. Chen, "Impacts of Tip Structure on RF-induced Heating of an Implantable Neurostimulator under 1.5 T

- MRI," 2018 IEEE Antennas Propag. Soc. Int. Symp. Usn. Natl. Radio Sci. Meet. APSURSI 2018 Proc., no. 1, pp. 2383–2384, 2018.
- [18] P. Serano, L. M. Angelone, H. Katnani, E. Eskandar, and G. Bonmassar, "A novel brain stimulation technology provides compatibility with MRI," Sci. Rep., vol. 5, pp. 1–10, 2015.
- [19] L. Golestanirad et al., "Reducing RF-Induced Heating Near Implanted Leads Through High-Dielectric Capacitive Bleeding of Current (CBLOC)," *IEEE Trans. Microw. Theory Tech.*, vol. 67, no. 3, pp. 1265–1273, 2019.
- [20] S. O. McCabe and J. B. Scott, "Cause and Amelioration of MRI-Induced Heating Through Medical Implant Lead Wires," 21st Electron. New Zeal. Conf., 2014.
- [21] R. Das and H. Yoo, "RF Heating Study of a New Medical Implant Lead for 1.5 T, 3 T, and 7 T MRI Systems," *IEEE Trans. Electromagn. Compat.*, vol. 59, no. 2, pp. 360–366, 2017.
- [22] R. W. Gray, W. T. Bibens, and F. G. Shellock, "Simple design changes to wires to substantially reduce MRI-induced heating at 1.5 T: Implications for implanted leads," *Magn. Reson. Imaging*, vol. 23, no. 8, pp. 887–891, 2005.
- [23] P. Nordbeck et al., "Reducing RF-related heating of cardiac pacemaker leads in MRI: Implementation and experimental verification of practical design changes," *Magn. Reson. Med.*, vol. 68, no. 6, pp. 1963– 1972, 2012.
- [24] S. Mccabe, and J. Scott, "A novel implant electrode design safe in the RF Field of MRI Scanners," *IEEE Trans. Microw. Theory Tech.*, vol. 65, no. 9, pp. 3541–3547, 2017.
- [25] R. Yang, J. Zheng, Y. Wang, R. Guo, W. Kainz, and J. Chen, "Impact of electrode structure on rf-induced heating for an aimd implanted lead in a 1.5-Tesla mri system," in *IEEE Journal of Electromagnetics, RF* and Microwaves in Medicine and Biology, 2019.
- [26] S. Feng, R. Qiang, W. Kainz, and J. Chen, "A technique to evaluate MRI-induced electric fields at the ends of practical implanted lead," *IEEE Trans. Microw. Theory Tech.*, vol. 63, no. 1, pp. 305–313, 2015.